Steady state evaluation of distributed secondary frequency control strategies for microgrids in the presence of clock drifts*

Ajay Krishna[1], Christian A. Hans[1], Johannes Schiffer[2], Jörg Raisch[1,3] and Thomas Kral[4]

***Abstract*— Secondary frequency control, i.e., the task of restoring the network frequency to its nominal value following a disturbance, is an important control objective in microgrids. In the present paper, we compare distributed secondary control strategies with regard to their behaviour under the explicit consideration of clock drifts. In particular we show that, if not considered in the tuning procedure, the presence of clock drifts may impair an accurate frequency restoration and power sharing. As a consequence, we derive tuning criteria such that zero steady state frequency deviation and power sharing is achieved even in the presence of clock drifts. Furthermore, the effects of clock drifts of the individual inverters on the different control strategies are discussed analytically and in a numerical case study.**

I. Introduction

Electric power systems are currently facing various challenges that mostly arise from an increase in spatially distributed renewable energy sources (RES). As a consequence, power generation is moving from a relatively small number of large scale power stations to a very large number of small scale distributed units. A promising way to tackle the challenges that arise from this structural change is the decomposition of the overall grid into regional entities called microgrids (MGs). MGs typically consist of renewable and storage units, as well as conventional generators, and loads. In a general setting, MGs may interact with each other, but - by matching generation and consumption within the MG as far as possible - transmitted power is reduced and transmission losses are decreased. MGs can usually be operated in two modes, either connected to the grid or electrically isolated (islanded) [1].

Motivated by existing control strategies in conventional power systems, a hierarchical control approach has also been advocated for MGs [2]. Thereby, one typically distinguishes primary and secondary control layers (as in conventional power systems), while the top control level, which is mostly referred to as operational management or tertiary control, is mainly concerned with generation scheduling.

*The project leading to this manuscript has received funding from the German Academic Exchange Service (DAAD), the German Federal Ministry for Economic Affairs and Energy (BMWi), Project No. 0325713A and the European Union's Horizon 2020 research and innovation programme under the Marie Skłodowska-Curie grant agreement No. 734832.

[1]Fachgebiet Regelungssysteme, Technische Universität Berlin, Germany, {krishna, hans, raisch}@control.tu-berlin.de

[2]School of Electronic and Electrical Engineering, University of Leeds, UK, j.schiffer@leeds.ac.uk

[3]Max-Planck-Institut für Dynamik komplexer technischer Systeme, Magdeburg, Germany

[4]Younicos AG, Berlin, Germany, thomas.kral@younicos.com

Primary control is typically implemented in the form of decentralised proportional (droop) control. Its major objectives are active power sharing as well as frequency and voltage stability [1]. In MGs, this task is mostly assigned to conventional generators and grid forming inverters [3]. Despite many advantages, a major drawback of this control law is that voltage amplitudes and frequencies usually deviate from their nominal values at steady state [4].

Secondary frequency control aims at removing stationary frequency deviations. There are two prominent implementation approaches: centralised and distributed controllers. Central approaches are widely used in existing power systems [5] and have been implemented and studied for MGs in [1], [2]. However, a major disadvantage of such approaches is that the central control unit represents a single point of failure. This issue motivated distributed strategies which use locally available as well as neighbouring information that is exchanged over a communication network [6].

Recently, various distributed secondary frequency control strategies have been proposed. A distributed averaging proportional integral secondary controller was presented in [7]. For this, an optimal tuning strategy using the input-output $\mathcal{H}_2$-norm has been provided by [8]. A related consensus based distributed frequency controller was proposed by [9]. Therein, a so called pinning control is used to ensure zero steady state frequency error. Another distributed frequency control approach is presented in [10]. Here also, pinning control is used to achieve frequency convergence. This way, the reference frequency value only needs to be provided for one inverter. Consensus based distributed frequency control along with a weight calculation procedure for optimal convergence speed is presented in [11]. All the above mentioned control laws can achieve frequency synchronisation. Furthermore, the communication layer can be designed such that the controllers are resilient to communication path failures. In [12], conditions for robust non-linear stability of MGs operated with a distributed averaging integral controller under fast-varying time-delays and switching communication topology are derived. Furthermore, various secondary frequency control policies are compared in [13]. In particular, the effects of communication properties on different strategies, such as, centralized, decentralized, averaging and consensus strategies, are analysed in a quantitative way.

In this work, we explicitly consider the effect of clock drifts in secondary frequency control. The term *clock drifts* describes the fact that all units, operated with different processors have a slightly different "understanding" of time, i.e., their clock rates are not synchronized [14]. Most of

the distributed control approaches, as they make use of the internal frequencies that are calculated by the controls of the inverters, are influenced by clock drifts. In practice, even if the units are synchronized to a global frequency, the internal frequencies of the inverters are slightly different [15]. As external synchronization units that could hamper this problem are expensive, they are not used in most of the applications. Whereas, a widely chosen alternative approach to tackle this problem is the use of a central secondary controller with a very accurate measurement. To enable a design of distributed controllers that fulfil the requirement of zero steady state frequency error and power sharing, conditions on the tuning in the presence of clock drifts must be derived. However, to the best knowledge of the authors, none of the publications on secondary frequency control investigates the effect of clock drifts.

Motivated by this fact, we compare a set of different distributed control strategies proposed in the literature [7], [10] with regard to their steady state performance in terms of frequency restoration and power sharing under explicit consideration of clock drifts. Furthermore, we identify a suitable parametrisation for a distributed control strategy that achieves zero steady state frequency error and steady state power sharing in the presence of clock drifts.

The remainder of this paper is structured as follows. In Section II, we provide the model for the electrical network and the distributed units. Then, in Section III a central and a distributed secondary frequency controller are introduced. In Section IV, the distributed controller is parametrized to resemble different control laws reported in the literature. These control laws are then analysed regarding their steady state behaviour. Finally, in Section V, we compare performance of the different controllers in a case study.

II. Model of a microgrid

In this section, the employed MG model is introduced. We start by introducing some notation and basics on graph theory.

A. Preliminaries and notations

Throughout the paper, the identity matrix of size $N \times N$ is denoted by $\mathbf{I}_N$. Furthermore, $\mathbf{1}_N \in \mathbb{R}^N$ is the vector of all ones and $\mathbf{0}_N \in \mathbb{R}^N$ is the vector of all zeros. The matrix of all ones is denoted by $\mathbf{1}_{N\times N} \in \mathbb{R}^{N\times N}$ and the matrix of all zeros by $\mathbf{0}_{N\times N} \in \mathbb{R}^{N\times N}$. The $N \times N$ diagonal matrix with entries a_j, $j = 1, \dots, N$ is denoted by $\operatorname{diag}(a_j)$.

1) Graph theory: A finite undirected graph $\mathcal{G}$ is a tuple $\mathcal{G} = (\mathcal{J}, \mathcal{E})$, where $\mathcal{J}$ is a finite set of vertices with $\mathcal{J} = \{1, \dots, J\}$ and $J \in \mathbb{N}$ is the total number of vertices. Furthermore, $\mathcal{E} \subseteq [\mathcal{J}]^2$ is the set of edges where $[\mathcal{J}]^2$ represents the set of all two-element subsets of $\mathcal{J}$. The entries of the adjacency matrix $A \in \mathbb{R}^{J\times J}$ of $\mathcal{G}$ are $a_{ij} = a_{ji} = 1$ if $\{i, j\} \in \mathcal{E}$ and $a_{ij} = a_{ji} = 0$ otherwise. The set of neighbouring nodes of node i is given by $\mathcal{J}_i = \{j \in \mathcal{J} \,|\, a_{ij} \neq 0\}$.

An ordered sequence of nodes such that any pair of consecutive nodes in the sequence is connected by an edge is called a path. If there exists a path between every pair of distinct nodes, then the graph $\mathcal{G}$ is called connected. The diagonal degree matrix $\mathcal{D} \in \mathbb{R}^{J\times J}$ is given by $\mathcal{D} = \operatorname{diag}\left(\sum_{j\in\mathcal{J}} a_{ij}\right)$. The Laplacian matrix $\mathcal{L} \in \mathbb{R}^{J\times J}$ of an undirected graph is given by $\mathcal{L} = \mathcal{D} - A$. If and only if a graph $\mathcal{G}$ is connected, then $\mathcal{L}$ is positive semi-definite, with a simple zero eigenvalue and a corresponding right eigenvector $\mathbf{1}_J$ [16]. Thus, $\mathcal{L}\mathbf{1}_J = \mathbf{0}_J$ and $\mathbf{1}_J^T\mathcal{L} = \mathbf{0}_J^T$ [17].

B. Network modelling

The electrical network of the considered microgrid is assumed to be connected. In this network, vertices at which only loads and no other units are connected, are called passive nodes. Using Kron-reduction [18], the original network containing passive nodes is reduced to a lower dimensional network that contains only nodes where grid forming units, i.e., grid forming inverters or rotating generators, are connected. We assume this reduction has been carried out. Then, each grid forming unit $i \in \mathcal{J}$ is connected to a node $i \in \mathcal{J}$. This work focusses on secondary frequency control. Therefore, we assume that the voltage amplitudes $V_i \in \mathbb{R}_{\geq 0}$ at all buses are constant [19].

Denoting the vector of phase angles of all nodes in the grid by $\delta = (\delta_1, \dots, \delta_J) \in \mathbb{R}^J$, the active power injection of unit i is given by

$$P_i(\delta) = G_{ii}V^2 + V^2 \sum_{j\in\mathcal{J}_i} |Y_{ij}| \sin\left(\delta_i - \delta_j + \phi_{ij}\right), \quad (1)$$

where $G_{ii} = \hat{G}_{ii} + \sum_{j=1, j\neq i}^{J} G_{ij}$. Here, $G_{ii} \in \mathbb{R}$ is the self-conductance, $\hat{G}_{ii} \in \mathbb{R}$ denotes the shunt conductance at node i and $G_{ij} \in \mathbb{R}_{\geq 0}$ the conductance of the line connecting nodes i and j [18]. With the susceptance $B_{ij} \in \mathbb{R}$, the absolute value of the admittance is given by $|Y_{ij}| = (G_{ij}^2 + B_{ij}^2)^{\frac{1}{2}}$. Moreover, $\phi_{ij} = \arctan\left(G_{ij}/B_{ij}\right)$ is the admittance angle. Note that if there is no direct electrical connection between nodes i and j then $Y_{ij} = 0$.

Usually, grid forming units such as synchronous generators and grid forming inverters are employed for frequency restoration. Also, all the loads and grid feeding units can be described by a constant impedance $G_{ii}V^2 \quad \forall i \in \mathcal{J}$. Therefore this work will focus on grid forming units which will be simply referred to as units in the following.

C. Droop controlled units

A widely used control approach in MGs is droop control, implemented on grid-forming inverters and synchronous generators. To realize this low level control, each unit is typically equipped with its own digital controller with individual processor clock. The time signal of *all* controllers slightly vary from each other because of the so called *clock drifts* [15]. As has been shown in [15], clock drifts can be incorporated in the model of a grid-forming inverter by introducing a (constant) unknown scaling factor in the model. Then, the dynamics of the ith unit equipped with frequency droop

control is given by

$$(1+\mu_i)\dot{\delta}_i = (1+\mu_i)\omega_i = \bar{\omega}_i, \tag{2a}$$
$$= \omega^d - k_i(P_i^m - P_i^d) + \xi_i, \tag{2b}$$
$$(1+\mu_i)\tau_i \dot{P}_i^m = -P_i^m + P_i, \tag{2c}$$

where $\mu_i \in \mathbb{R}$, is the clock drift factor, $\omega_i \in \mathbb{R}$ is the actual electrical frequency and $\bar{\omega}_i \in \mathbb{R}$ is the internal frequency of the ith unit. Note that only the internal frequency $\bar{\omega}_i$ is available to every unit. Furthermore, $\omega^d \in \mathbb{R}$ is the frequency set point, $k_i \in \mathbb{R}_{>0}$ the droop coefficient, $P_i^d \in \mathbb{R}$ the active power set point from a higher control level, e.g, energy management [20], and $\xi_i \in \mathbb{R}$ is the control input. The measured active power $P_i^m \in \mathbb{R}$ is obtained by filtering the power output P_i in (1) by a first order low pass filter with time constant $\tau_i \in \mathbb{R}_{>0}$.

The model (2) can be used to model both, droop controlled inverters and synchronous generators (see, e.g., [21]). However, using (2) without any secondary control, i.e., $\xi_i = 0$, the steady state frequency error is typically non-zero. To achieve the desired $\bar{\omega}_i = \omega^d$, secondary control as described in the next section can be used.

III. Secondary frequency control

Secondary frequency control aims at driving the frequency value at steady state to a desired value. Strategies, that change the input ξ_i to achieve this goal are introduced in this section. The study starts with a widely used central control scheme. Then, a distributed secondary control law is presented.

A. Central control

A standard approach for frequency secondary control is to measure the frequency at a single bus bar where an accurate frequency measurement can be realised. This frequency value is then used in a standard central frequency controller (see, e.g., [5]). Such control law can be described by

$$\dot{\xi}_c = \omega_d - \omega_c, \quad \xi_i = b_i \xi_c, \quad \forall i \in \mathcal{J}, \tag{3}$$

where $\xi_c \in \mathbb{R}$ is the integrated frequency error and ω_c is the frequency measured at one bus, $\xi_i \in \mathbb{R}$ is the secondary control input and $b_i \in \mathbb{R}_{\geq 0}$ is the controller gain of unit i.

Usually in this control scheme, clock drifts are addressed using an accurate central frequency measurement with $\mu_c = 0$ and hence, $\bar{\omega}_c = \omega_c$. Despite their popularity, central controllers are vulnerable to single point failures which need to be addressed by redundant communication or computation infrastructure [10].

B. Distributed consensus based control

A generalised representation of a consensus based distributed secondary frequency control scheme explicitly considering clock drifts is

$$(1+\mu_i)\dot{\xi}_i = -\big(b_i(\bar{\omega}_i - \omega^d) + c_i \textstyle\sum_{j\in\mathcal{J}_{\mathcal{G}_i}} a_{ij}(\bar{\omega}_i - \bar{\omega}_j) + d_i \sum_{j\in\mathcal{J}_{\mathcal{G}_i}} a_{ij}(\xi_i - \xi_j)\big), \tag{4}$$

where $b_i \in \mathbb{R}$ is called pinning gain and $c_i \in \mathbb{R}$ as well as $d_i \in \mathbb{R}$ are controller gains. Furthermore, $a_{ij} \in \mathbb{R}_{\geq 0}$ are entries from the adjacency matrix (see Section II-A) that describes the communication structure of the secondary controller and $\mathcal{J}_{\mathcal{G}_i}$ is the set of neighbouring units of unit i for the communication network. By parametrising (4), different control strategies can be implemented, e.g., [10], [7] or a controller similar to the one described by [9]. For all considered strategies, we assume the communication graph is connected and undirected.

Combining the unit model (2) with the power flow equations (1) and the distributed control (4), the dynamics of the closed-loop MG system can be written as

$$(\mathbf{I}_J + \mu)\dot{\delta} = (\mathbf{I}_J + \mu)\omega = \bar{\omega}, \tag{5a}$$
$$= \mathbf{1}_J \omega^d - \mathbf{k}(P^m - P^d) + \xi, \tag{5b}$$
$$(\mathbf{I}_J + \mu)\tau \dot{P}^m = -P^m + P(\delta), \tag{5c}$$
$$(\mathbf{I}_J + \mu)\dot{\xi} = -\big((\mathbf{B} + \mathbf{C}\mathcal{L})(\bar{\omega} - \mathbf{1}_J\omega^d) + \mathbf{D}\mathcal{L}\xi\big), \tag{5d}$$

where

$$\mu = \mathrm{diag}(\mu_1, \ldots, \mu_J), \qquad \xi = [\xi_1, \ldots, \xi_J]^T,$$
$$\omega = [\omega_1, \ldots, \omega_J]^T, \qquad \tau = \mathrm{diag}(\tau_1, \ldots, \tau_J),$$
$$\bar{\omega} = [\bar{\omega}_1, \ldots, \bar{\omega}_J]^T, \qquad P(\delta) = [P_1(\delta), \ldots, P_J(\delta)]^T,$$
$$\mathbf{k} = \mathrm{diag}(k_1, \ldots, k_J), \qquad \mathbf{B} = \mathrm{diag}(b_1, \ldots, b_J),$$
$$P^d = [P_1^d, \ldots, P_J^d]^T, \qquad \mathbf{C} = \mathrm{diag}(c_1, \ldots, c_J),$$
$$P^m = [P_1^m, \ldots, P_J^m]^T, \qquad \mathbf{D} = \mathrm{diag}(d_1, \ldots, d_J).$$

Note that (5) is non-linear due to $P(\delta)$ from (1). For the subsequent analysis, it is convenient to introduce the notion below.

Definition 1: The system (5) admits a synchronised motion if it has a solution for all $t \geq 0$ of the form

$$\delta^s(t) = \delta_0^s + \omega^s t, \quad \omega^s = \mathbf{1}_J \omega^*, \tag{6a}$$

with $\omega^* \in \mathbb{R}$ and $\delta_0^s \in \mathbb{R}^J$ such that

$$|\delta_{0,i}^s - \delta_{0,j}^s| < \frac{\pi}{2} \quad \forall \quad i \in \mathcal{J},\ j \in \mathcal{J}_i. \tag{6b}$$

With Definition 1, we can now analyse the steady state behaviour of the closed-loop system (5) for different parametrisations of the controller (4) in the next section.

IV. Steady-state behaviour of distributed secondary control strategies

The control strategies described in Section IV aim at driving the steady state error of the frequency to zero. In this section we will analyse under which parametrization of the control (4), this can be achieved. Furthermore, we will investigate how power sharing, i.e., that the units share variations in load power in a desired manner, can be ensured. Before analysing these properties, we derive an analytic expression for the steady state frequency and a condition for power sharing.

Lemma 1: Suppose that (5) admits a synchronised motion (see Definition 1) where $\mathbf{D}$ is non-singular and that at least one of the matrices $\mathbf{B}$ and $\mathbf{C}$ is non-zero. Then, the corresponding synchronised electrical frequency is given by

$$\omega^* = \frac{\mathbf{1}_J^T \mathbf{D}^{-1} \mathbf{B} \mathbf{1}_J}{\mathbf{1}_J^T \mathbf{D}^{-1}(\mathbf{B} + \mathbf{C}\mathcal{L})(\mathbf{I}_J + \mu)\mathbf{1}_J} \omega^d. \tag{7}$$

Furthermore, $\omega^* = \omega^d$ if and only if

$$\mathbf{1}_J^T \mathbf{D}^{-1}(\mathbf{B} + \mathbf{C}\mathcal{L})\mu \mathbf{1}_J = 0. \tag{8}$$

Proof: Along any synchronised motion, the electrical frequencies at all nodes of (5) have to be identical, i.e.,

$$\dot{\delta}^s = \omega^s = \mathbf{1}_J \omega^*, \tag{9}$$

which directly implies from (5a) that

$$\bar{\omega}^s = (\mathbf{I}_J + \mu)\mathbf{1}_J \omega^*. \tag{10}$$

Furthermore, $\dot{\xi}^s = \mathbf{0}_J$. Hence,

$$(\mathbf{I}_J + \mu)\dot{\xi}^s = \mathbf{0}_J = (\mathbf{B} + \mathbf{C}\mathcal{L})(\bar{\omega}^{\mathbf{s}} - \mathbf{1}_J \omega^d) + \mathbf{D}\mathcal{L}\xi^s. \tag{11}$$

Multiplying (11) from the left with $\mathbf{1}_J^T \mathbf{D}^{-1}$ and recalling the fact from Section II-A that $\mathbf{1}_J^T \mathcal{L} = \mathbf{0}_J^T$ as the graph induced by the communication network is undirected and connected yields

$$0 = \mathbf{1}_J^T \mathbf{D}^{-1}(\mathbf{B} + \mathbf{C}\mathcal{L})(\bar{\omega}^{\mathbf{s}} - \mathbf{1}_J \omega^d).$$

Using (10) and $\mathcal{L}\mathbf{1}_J = \mathbf{0}_J$ leads to

$$0 = \mathbf{1}_J^T \mathbf{D}^{-1} \left((\mathbf{B} + \mathbf{C}\mathcal{L})(\mathbf{I}_J + \mu)\mathbf{1}_J \omega^* - \mathbf{B}\mathbf{1}_J \omega^d \right).$$

Unless $\mathbf{B} = \mathbf{0}_{J\times J}$ or $\omega^d = 0$, the above equation is solvable if $\mathbf{1}_J^T \mathbf{D}^{-1}(\mathbf{B}+\mathbf{C}\mathcal{L})(\mathbf{I}_J+\mu)\mathbf{1}_J$ is non-zero. Then, (7) follows immediately.

To show that $\omega^* = \omega^d$ if and only if (8) is satisfied, we note that according to (7), $\omega^* = \omega^d$ if and only if

$$\mathbf{1}_J^T \mathbf{D}^{-1}(\mathbf{B} + \mathbf{C}\mathcal{L})(\mathbf{I}_J + \mu)\mathbf{1}_J = \mathbf{1}_J^T \mathbf{D}^{-1}\mathbf{B}\mathbf{1}_J.$$

Recalling the fact that $\mathbf{C}\mathcal{L}\mathbf{1}_J = \mathbf{0}_J$, the above equation is equivalent to (8). ∎

Next, we investigate under which conditions power sharing can be achieved with the control (4) in the presence of clock drifts. In this work, we are interested in power sharing relative to the set-points P_i^d. Therefore, we employ the definition below, which is in a similar spirit to that introduced in [21].

Definition 2: Let $\chi_i \in \mathbb{R}_{>0}$ and $\chi_j \in \mathbb{R}_{>0}$. The units at nodes $i \in \mathcal{J}$ and $j \in \mathcal{J}$ share their active powers proportionally if

$$\frac{P_i^s - P_i^d}{\chi_i} = \frac{P_j^s - P_j^d}{\chi_j}. \tag{12}$$

In vector notation with $\mathcal{X} = \operatorname{diag}(\chi_1, \ldots, \chi_J)$ and any arbitrary constant $\gamma \in \mathbb{R}$, (12) can be expressed as $\mathcal{X}^{-1}(P^s - P^d) = \gamma \mathbf{1}_J$. Note that χ_i and χ_j are parameters that can be chosen by the designer and don't necessarily have to be equal. In practice, a typical choice for χ_i is the nominal power rating of the unit at node i.

Lemma 2: Assume that the system (5) possesses a synchronized motion (see Definition 1). Then, active power sharing along this motion can be achieved if and only if $\mathbf{k}$, $\mathbf{B}$, $\mathbf{C}$ and $\mathbf{D}$ are chosen such that

$$\big(\mathbf{B} + (\mathbf{C} + \mathbf{D})\mathcal{L}\big)\mathbf{F}\mathbf{1}_J \omega^d + \gamma \mathbf{D}\mathcal{L}\mathbf{k}\mathcal{X}\mathbf{1}_J = \mathbf{0}_J, \tag{13}$$

where

$$\mathbf{F} = \frac{\mathbf{1}_J^T \mathbf{D}^{-1}\mathbf{B}\mathbf{1}_J}{\mathbf{1}_J^T \mathbf{D}^{-1}(\mathbf{B}+\mathbf{C}\mathcal{L})(\mathbf{I}_J+\mu)\mathbf{1}_J}(\mathbf{I}_J + \mu) - \mathbf{I}_J. \tag{14}$$

Proof: Along a synchronised motion, (5) becomes

$$\bar{\omega}^s = \mathbf{1}_J \omega^d - \mathbf{k}(P^m - P^d) + \xi^s, \tag{15a}$$

$$\mathbf{0}_J = -P^m + P^s, \tag{15b}$$

$$\mathbf{0}_J = (\mathbf{B} + \mathbf{C}\mathcal{L})(\bar{\omega}^{\mathbf{s}} - \mathbf{1}_J \omega^d) + \mathbf{D}\mathcal{L}\xi^s. \tag{15c}$$

Using (15b), we can rewrite (15a) as

$$\xi^s = (\bar{\omega}^s - \mathbf{1}_J \omega^d) + \mathbf{k}(P^s - P^d).$$

Inserting this equation in (15c) results in

$$\mathbf{0}_J = \big(\mathbf{B} + (\mathbf{C} + \mathbf{D})\mathcal{L}\big)(\bar{\omega}^s - \mathbf{1}_J \omega^d) + \mathbf{D}\mathcal{L}\mathbf{k}(P^s - P^d).$$

Following Definition 2, with $P^s - P^d = \gamma \mathcal{X}\mathbf{1}_J$, we have

$$\mathbf{0}_J = \big(\mathbf{B} + (\mathbf{C} + \mathbf{D})\mathcal{L}\big)(\bar{\omega}^s - \mathbf{1}_J \omega^d) + \gamma \mathbf{D}\mathcal{L}\mathbf{k}\mathcal{X}\mathbf{1}_J.$$

Furthermore, using (10) yields

$$\mathbf{0}_J = \big(\mathbf{B} + (\mathbf{C} + \mathbf{D})\mathcal{L}\big)\big((\mathbf{I}_J + \mu)\mathbf{1}_J \omega^* - \mathbf{1}_J \omega^d\big) + \gamma \mathbf{D}\mathcal{L}\mathbf{k}\mathcal{X}\mathbf{1}_J. \tag{16}$$

Substituting (7), power sharing is achieved if and only if

$$\big(\mathbf{B} + (\mathbf{C} + \mathbf{D})\mathcal{L}\big)\mathbf{F}\mathbf{1}_J \omega^d + \gamma \mathbf{D}\mathcal{L}\mathbf{k}\mathcal{X}\mathbf{1}_J = \mathbf{0}_J,$$

with $\mathbf{F}$ given in (14), completing the proof. ∎

Since the coefficients μ_i are unknown, Lemma 2 reveals that unlike in the case of ideal clocks [9], [7], [10], when taking clock drifts explicitly into account, it is hard to derive necessary and sufficient conditions for the controller gains $\mathbf{B}$, $\mathbf{C}$, $\mathbf{D}$ and $\mathbf{k}$ to guarantee power sharing. However, based on Lemmata 1 and 2 we can provide the following tuning criterion that ensures power sharing.

Lemma 3: Assume that the system (5) possesses a synchronized motion (see Definition 1). Then, active power sharing along this motion can be achieved if $\mathbf{k}$, $\mathbf{B}$, $\mathbf{C}$ and $\mathbf{D}$ are chosen such that

$$\mathbf{B}\mu = \mathbf{0}_{J\times J}, \text{ and } (\mathbf{C} + \mathbf{D}) = \mathbf{0}_{J\times J}, \tag{17a}$$

as well as

$$\mathbf{k}\mathcal{X} = \alpha \mathbf{I}_J \tag{17b}$$

with $\alpha \in \mathbb{R}$.

Proof: For $\mathbf{B}\mu = \mathbf{0}_{J\times J}$, (8) becomes

$$\mathbf{1}_J^T \mathbf{D}^{-1}\mathbf{C}\mathcal{L}\mu \mathbf{1}_J = 0.$$

Furthermore, with $(\mathbf{C} + \mathbf{D}) = \mathbf{0}_{J\times J} \Leftrightarrow \mathbf{D}^{-1}\mathbf{C} = -\mathbf{I}_J$, and recalling the fact that $\mathbf{1}_J^T \mathcal{L} = \mathbf{0}_J$, we can show that (8) holds. Thus, $\omega^* = \omega^d$ if (17a) holds. Furthermore, with $\mathbf{B}\mu = \mathbf{0}_J$ and $(\mathbf{C} + \mathbf{D}) = \mathbf{0}_{J\times J}$,(13) becomes

$$\mathbf{0}_J = \gamma \mathbf{D}\mathcal{L}\mathbf{k}\mathcal{X}\mathbf{1}_J.$$

Inserting (17b) yields

$$\mathbf{0}_J = \gamma\alpha \mathbf{D}\mathcal{L}\mathbf{1}_J.$$

This completes the proof. ∎

Using the derived conditions from Lemmata 1–3, in the following we will investigate whether and how a zero steady state frequency error and power sharing can be reached. Therefore, we will compare different parametrizations of the control law (4).

A. Pinning gain at all units, no consensus-based exchange of internal frequencies

By setting $b_i > 0$, $c_i = 0$ and $d_i > 0$ for all $i \in \mathcal{J}$ the control law (4) becomes

$$(1+\mu_i)\dot{\xi}_i = -\big(b_i(\bar{\omega}_i-\omega^d)+d_i\textstyle\sum_{j\in\mathcal{J}_{\mathcal{G}_i}} a_{ij}(\xi_i-\xi_j)\big), \quad (18)$$

which is equal to the secondary control scheme proposed in [7]. In this strategy, the internal frequencies of all units are used in the first term with the pinning gain. Consensus-based exchange of the internal frequencies is not included, i.e., $\mathbf{C} = \mathbf{0}_{J\times J}$. Thus, supposing that the system (5) admits a synchronised motion, condition (8) in Lemma 1 reduces to

$$\mathbf{1}_J^T\mathbf{D}^{-1}\mathbf{B}\mu\mathbf{1}_J = 0. \quad (19)$$

The clock drift factors μ_i for $i \in \mathcal{J}$ are uncertain. Usually, $\mu_i \neq \mu_j \neq 0$ for $i, j \in \mathcal{J}$, $i \neq j$ holds. In (18), as $\mathbf{D}^{-1}$ and $\mathbf{B}$ are positive-definite, condition (19) cannot be satisfied. Hence, due to the impact of clock drifts, frequency convergence (i.e, $\omega^* = \omega^d$) cannot be achieved with the control law (18). Furthermore, (17a) does not hold, as $(\mathbf{C}+\mathbf{D}) \neq \mathbf{0}_{J\times J}$ and $\mathbf{B}\mu \neq \mathbf{0}_{J\times J}$. Therefore, active power sharing cannot be ensured.

B. Pinning gain at one unit, no consensus-based exchange of internal frequencies

In this approach, (4) is parametrized by setting the pinning gain $b_i = 0$ for all units $i \in \mathcal{J} \setminus \{k\}$ except for unit $k \in \mathcal{J}$ where $b_k > 0$. This unit k is assumed to have access to accurate frequency measurement with $\mu_k = 0$. Furthermore, $c_i = 0$ and $d_i > 0$ for all $i \in \mathcal{J}$. Hence, the control law (4) reduces to

$$(1+\mu_i)\dot{\xi}_i = -\big(b_i(\bar{\omega}_i-\omega^d)+d_i\textstyle\sum_{j\in\mathcal{J}_{\mathcal{G}_i}} a_{ij}(\xi_i-\xi_j)\big), \quad (20)$$

and thus is equivalent to the one proposed in [10] as shown in Appendix I. Assuming a synchronised motion (see Definition 1) and using $\mathbf{C} = \mathbf{0}_{J\times J}$, the convergence condition (8) reduces to

$$\mathbf{1}_J^T\mathbf{D}^{-1}\mathbf{B}\mu\mathbf{1}_J = 0. \quad (21)$$

Since b_i is zero for all $i \in \mathcal{J} \setminus \{k\}$ and $\mu_k = 0$ for the kth controller, $\mathbf{B}\mu = \mathbf{0}_{J\times J}$. Thus, (8) holds and $\omega^* = \omega^d$ in steady state.

To investigate power sharing, we note that $\mathbf{B}\mu = \mathbf{0}_{J\times J}$ and $\mathbf{C} = \mathbf{0}_{J\times J}$. Thus, (13) and (14) can be combined and reduces to

$$(\mathbf{B}+\mathbf{D}\mathcal{L})\mu\mathbf{1}_J\omega^d + \gamma\mathbf{D}\mathcal{L}\mathbf{k}\mathcal{X}\mathbf{1}_J = \mathbf{0}_J.$$

Again using the fact that $\mathbf{B}\mu = \mathbf{0}_{J\times J}$ yields

$$\mathbf{D}\mathcal{L}\mu\mathbf{1}_J\omega^d + \gamma\mathbf{D}\mathcal{L}\mathbf{k}\mathcal{X}\mathbf{1}_J = \mathbf{0}_J.$$

However, it remains difficult to derive any conditions on the choice of $\mathbf{D}$ that ensures power sharing. Hence, the approach presented in (20) partially fulfils the control objectives as a zero steady state frequency error can be reached. However, power sharing cannot be guaranteed.

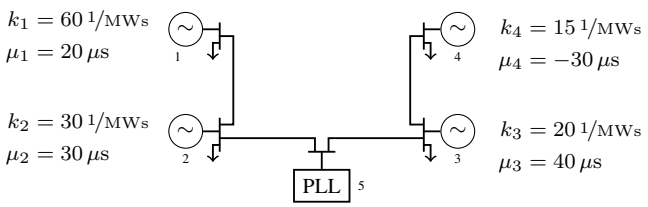

Fig. 1: MG used in case study.

C. Pinning gain at one unit, with consensus-based exchange of internal frequencies

Similar to the approach in Section IV-B, (4) is parametrized such that $b_k > 0$ at one unit k with an accurate frequency measurement, i.e., $\mu_k = 0$. For all other units $i \in \mathcal{J} \setminus \{k\}$, $b_i = 0$. Furthermore, $d_i > 0$ for all $i \in \mathcal{J}$. Note that the consensus-based exchange of internal frequencies is allowed, i.e, $\mathbf{C}$ may be non-zero. The resulting controller has the form

$$\begin{aligned}(1+\mu_i)\dot{\xi}_i = -\big(&b_i(\bar{\omega}_i-\omega^d)+\\ &c_i\textstyle\sum_{j\in\mathcal{J}_{\mathcal{G}_i}} a_{ij}(\bar{\omega}_i-\bar{\omega}_j) + d_i\sum_{j\in\mathcal{J}_{\mathcal{G}_i}} a_{ij}(\xi_i-\xi_j)\big). \quad (22)\end{aligned}$$

Assuming existence of a synchronized motion and recalling $\mathbf{B}\mu = \mathbf{0}_{J\times J}$, (8) becomes

$$\mathbf{1}_J^T\mathbf{D}^{-1}\mathbf{C}\mathcal{L}\mu\mathbf{1}_J = 0, \quad (23)$$

along that synchronized motion. Selecting the matrices $\mathbf{C}$ and $\mathbf{D}$ such that

$$\mathbf{D}^{-1}\mathbf{C} = \rho\mathbf{I}_J, \quad (24)$$

with $\rho \in \mathbb{R}$, (23) holds, and therefore $\omega^* = \omega^d$. Thus for $\mathbf{C} = \rho\mathbf{D}$, a zero steady state frequency error can be achieved.

The power sharing condition (13) for the controller (22) with $\mathbf{B}\mu = \mathbf{0}_{J\times J}$ is given by

$$\big(\mathbf{B}+(\mathbf{C}+\mathbf{D})\mathcal{L}\big)\mathbf{F}\mathbf{1}_J\omega^d + \gamma\mathbf{D}\mathcal{L}\mathbf{k}\mathcal{X}\mathbf{1}_J = \mathbf{0}_J, \quad (25)$$

where

$$\mathbf{F} = \tfrac{\mathbf{1}_J^T\mathbf{D}^{-1}\mathbf{B}\mathbf{1}_J}{\mathbf{1}_J^T\mathbf{D}^{-1}\mathbf{B}\mathbf{1}_J+\mathbf{1}_J^T\mathbf{D}^{-1}\mathbf{C}\mathcal{L}\mu\mathbf{1}_J}(\mathbf{I}_J+\mu) - \mathbf{I}_J. \quad (26)$$

The condition (25) is satisfied if $\mathbf{D}^{-1}\mathbf{C} = -\mathbf{I}_J$, which in turn satisfies Lemma 3. Therefore substituting $\rho = -1$ in (24) will assure both zero steady state frequency error and power sharing for the controller (22).

Having achieved conditions for zero steady state frequency error and power sharing, in the following case study they will be illustrated for an exemplary microgrid. Therefore, the different parametrizations of (4) will be compared with each other and with the central controller (3).

V. Case study

In this section, the behaviour of the different approaches from Section IV is analysed exemplarily. First, we will introduce the MG used and the course of external actions in the simulation. Then, the operation of the grid with the different controllers is discussed.

A. Simulation setup

The case study was performed using MATLAB®/Simulink® and PLECS [22]. The structure of the MG used was motivated by the case studies of [7], [9], [10]. More specifically, the choice of the parameters is closely connected the ones used in [9]. As shown in Fig. 1, the MG consists of four units with different power ratings and loads. Motivated by [9], for all units $i \in \mathcal{J}$ with $\mathcal{J} = \{1, 2, 3, 4\}$, a time constant of $\tau_i = 0.16\,\mathrm{s}$ and the droop gains k_i as indicated in Fig. 1 were used. Furthermore, the desired power sharing was chosen as ${}^{1}/_{\chi_i} = k_i$ for all $i \in \mathcal{J}$. The clock drift factors μ_i were not part of the original model and introduced as shown in Fig. 1. Initially, a load of $(100 + \mathrm{j}\,100)\Omega$ is connected at each unit bus. The line parameters are the same as in [9], except for the following modification. The original MG, has a line that directly connects node 2 and 3. In our example, the line, i.e, the admittance of the line, was divided into two parts that connect node 2, respectively 3 with node 5. This was done to introduce a busbar where an accurate central frequency measurement, e.g., with a phase locked loop (PLL), can be performed. The course of external events of every simulation instance is described in Table I.

B. Central control

For the central controller, $b_i = 1$ for all $i \in \mathcal{J}$. Furthermore, the communication structure in Fig. 2a was used, i.e., the frequency is measured at the busbar (node c) and controlled according to (3). The communication in this case is directed from the central node to different units. In the beginning, there is a non-zero frequency error (see Fig. 3a). As the controller is enabled at $t = 10\,\mathrm{s}$, the error reduces to zero and the frequency is restored to 50 Hz (see magnified plot for frequency). The steady state frequency error also goes to zero after a change in active power at $t = 30\,\mathrm{s}$ occurs (see the bus bar frequency). However, power sharing at steady state is not achieved with this control strategy (see magnified plot for ${}^{P_i}/_{\chi_i}$).

C. Distributed consensus based control

The distributed secondary frequency control strategies were implemented and analysed with the MG and communication as in Fig. 2b. Thus, the busbar (node c) is not included in the secondary control and just serves for an accurate frequency measurement with $\mu_c = 0$.

TABLE I: Simulation scenario.

Time	Event
0 s	Start of simulation, primary control is activated;
10 s	Secondary control is activated;
30 s	Load with apparent power $S = 10\,\mathrm{kVA}$ and power factor $\cos(\phi) = 0.9$ (ind.) added to node 4;
70 s	Load with apparent power $S = 10\,\mathrm{kVA}$ and power factor $\cos(\phi) = 0.9$ (ind.) added to node 4;
90 s	End of simulation;

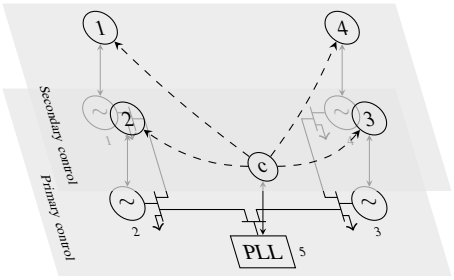

(a) Central integral secondary controller.

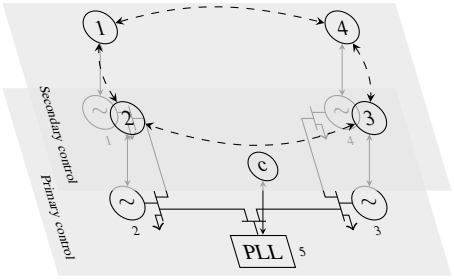

(b) Distributed integral secondary controller.

Fig. 2: Control layers of different controllers.

1) Pinning gain at all units, no consensus-based exchange of internal frequencies: Fig. 3b shows the output of approach (18) with $\mathbf{B} = \mathrm{diag}\,(\mathbf{1}_4)$, $\mathbf{C} = \mathrm{diag}\,(\mathbf{0}_4)$ and $\mathbf{D} = \mathrm{diag}\,(\mathbf{1}_4)$. It can be seen that the frequency that is measured accurately at the busbar is not exactly 50 Hz. Hence, as indicated in Section IV-A, a zero steady state frequency error is hard to reach with this strategy. At steady state, the power sharing is not achieved (see magnified plot for ${}^{P_i}/_{\chi_i}$) either.

2) Pinning gain at one unit, no consensus-based exchange of internal frequencies: In contrast to Fig. 1, in this approach unit 1 is assumed to have a very accurate clock (i.e., $\mu_1 = 0$). The rest of the clock drift factors μ_i for $i \in \mathcal{J} \setminus \{1\}$ remain unchanged. The controller parameters are assumed as $\mathbf{B} = \mathrm{diag}\,(1, 0, 0, 0)$, $\mathbf{C} = \mathrm{diag}\,(\mathbf{0}_4)$, and $\mathbf{D} = \mathrm{diag}\,(\mathbf{1}_4)$. Fig. 3c depicts the internal frequencies and active power ratios of the MG, controlled with strategy (20). It can be observed that the steady state frequency error of unit 1 and at the busbar goes to zero. Thus, as expected from Section IV-B, zero steady state frequency error is achieved. However, power sharing is not achieved.

3) Pinning gain at one unit, with consensus-based exchange of internal frequencies: In this approach, it is assumed that in contrast to Fig. 1, unit 1 incorporates a very accurate clock (i.e., $\mu_1 = 0$). The controller parameters are $\mathbf{B} = \mathrm{diag}\,(1, 0, 0, 0)$, $\mathbf{C} = \mathrm{diag}\,(-\mathbf{1}_4)$, and $\mathbf{D} = \mathrm{diag}\,(\mathbf{1}_4)$. Fig. 3d shows the simulation output of control strategy (22). It can be observed that the internal frequency at unit 1 coincides with the very accurate busbar frequency. Further, the theoretical results from the steady state analysis in Section IV-C could be reproduced, as a zero steady state frequency error as well as power sharing is achieved

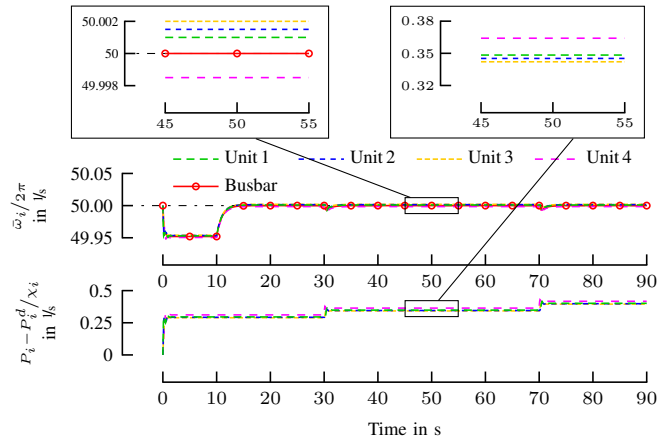

(a) Central controller (3).

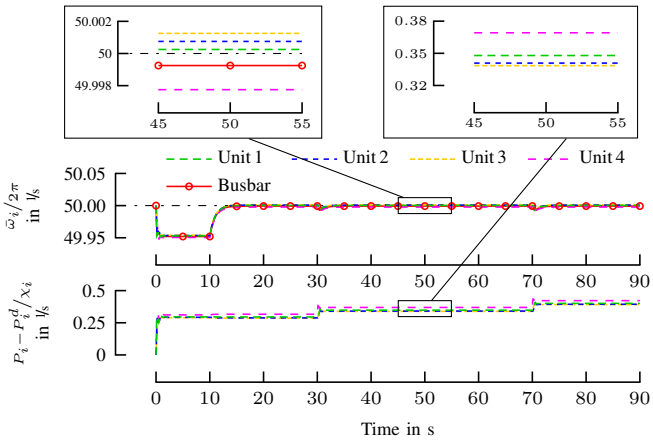

(b) Distributed controller (18) with pinning gain at all units, no consensus-based exchange of internal frequencies.

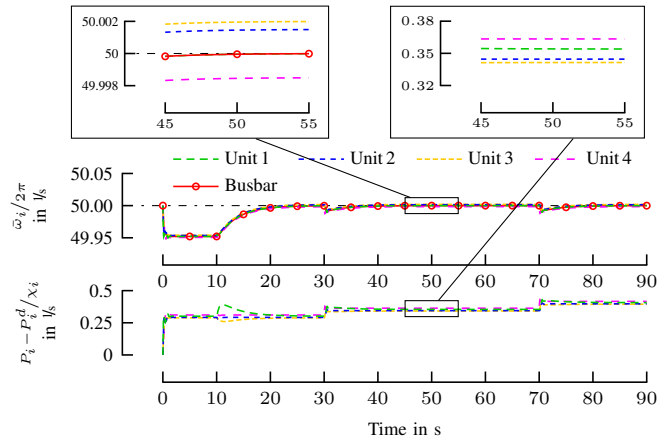

(c) Distributed controller (20) with pinning gain at one unit, no consensus-based exchange of internal frequencies.

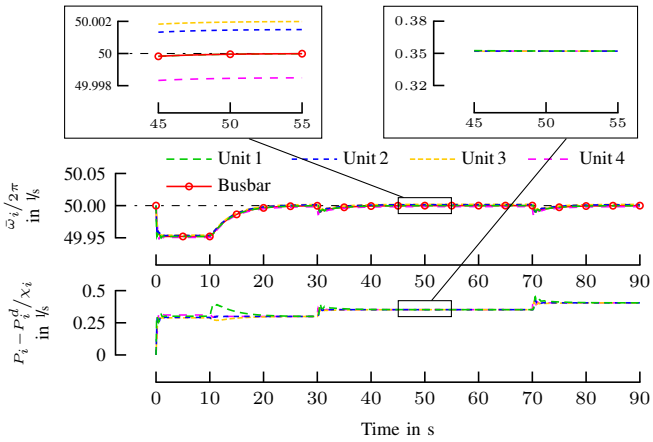

(d) Distributed controller (22) with pinning gain at one unit, with consensus-based exchange of internal frequencies.

Fig. 3: Frequency and active power ratios P_i/χ_i of MG operated with different controllers.

D. Comparison

The central controller (3) as per Fig. 3a has the capability to address clock drifts due to the presence of an accurate frequency measurement at the bus bar. However, power sharing is not achieved. Furthermore, since (3) is a central controller, it is prone to single point failures [1]. The distributed approaches in contrast can be designed in a way that is robust to those failures. Fig. 3b indicates that a zero steady state frequency error is hard to be achieved with (18). Control approaches that use a very accurate central frequency measurement at a node with non-zero pinning gain as in (20) and (22) are able to realise zero steady state frequency error in the presence of clock drifts. In steady state, power sharing can be achieved by using a distributed frequency secondary control that is parametrized as described in Section IV-C.

A brief overview of the applicability of the different approaches is also given in Table II. From this comparison, especially (22) seems to be a good choice because of zero frequency error and power sharing at steady state.

Remark 1: The control approaches (20) and (22) can also be implemented with central frequency measurement at a bus bar. Then, the busbar is added to the secondary control layer and the frequency reference ω^d is provided only to the busbar. The frequency at the busbar can be measured using, e.g., a PLL with very accurate clock signal or a power quality monitor.

VI. Conclusions

In this paper, the steady state behaviour of different secondary frequency controllers has been compared in the presence of clock drifts. A controller was proposed that uses

TABLE II: Comparison of different approaches.

Criterion	(3)	(18)	(20)	(22)
Zero steady state frequency error	✓		✓	✓
Steady state power sharing				✓
Central frequency measurement	✓		✓	✓
External frequency measurement possible	✓		✓	✓
Resilience to single-point failures possible by design		✓	✓	✓

an accurate frequency measurement at only one unit. With this controller, zero steady state frequency error and power sharing can be achieved. Sufficient conditions for zero steady state frequency deviation and power sharing for distributed secondary frequency control approaches have been derived. In a case study, the results from the analysis were illustrated and some practical aspects were discussed. Future work will address tuning of the different approaches for comparing their dynamic behaviour and to provide a stability proof for the proposed control approach. Furthermore, experiments in a real MG are planned.

REFERENCES

[1] J. A. P. Lopes, C. L. Moreira, and A. G. Madureira, "Defining control strategies for microgrids islanded operation," *IEEE Trans. Power Syst.*, 2006.

[2] J. M. Guerrero, P. Loh, M. Chandorkar, and T. Lee, "Advanced control architectures for intelligent microgrids - part 1 : Decentralized and hierarchial control," *IEEE Trans. Ind. Electron.*, vol. 60, no. 4, pp. 1254–1262, 2013.

[3] J. Rocabert, A. Luna, F. Blaabjerg, and P. Rodríguez, "Control of power converters in AC microgrids," *IEEE Trans. Power Electron.*, vol. 27, no. 11, pp. 4734–4749, 2012.

[4] M. C. Chandorkar, D. M. Divan, and R. Adapa, "Control of parallel connected inverters in standalone AC supply systems," *IEEE Trans. Ind. Appl.*, 1993.

[5] J. Machowski, J. Bialek, and J. Bumby, *Power systems dynamics : stability and control*, 2nd ed. Wiley, 2008.

[6] Q. Shafiee, M. Guerrero, and J. C. Vasquez, "Distributed secondary control for islanded microgrids- a novel approach," *IEEE Trans. Power Electron.*, 2014.

[7] J. W. Simpson-Porco, Q. Shafiee, F. Dörfler, J. C. Vasquez, J. M. Guerrero, and F. Bullo, "Secondary frequency and voltage control of islanded microgrids via distributed averaging," *IEEE Trans. Ind. Electron.*, vol. 62, pp. 7025–7038, 2015.

[8] E. Tegling, M. Andreasson, J. W. Simpson-Porco, and H. Sandberg, "Improving performance of droop-controlled microgrids through distributed pi-control," in *ACC*, July 2016, pp. 2321–2327.

[9] F. Guo, C. Wen, J. Mao, and Y. D. Song, "Distributed secondary voltage and frequency restoration control of droop-controlled inverter-based microgrids," *IEEE Trans. Ind. Electron.*, vol. 62, pp. 4355–4368, 2015.

[10] A. Bidram, F. L. Lewis, and A. Davoudi, "Distributed control systems for small-scale power networks," *IEEE Control Syst. Mag.*, 2014.

[11] D. Wu, T. Dragicevic, J. C. Vasquez, J. M. Guerrero, and Y. Guan, "Secondary coordinated control of islanded microgrids based on consensus algorithms," in *IEEE ECCE*, 2014, pp. 4290–4297.

[12] J. Schiffer, F. Dörfler, and E. Fridman, "Robustness of distributed averaging control in power systems: Time delays & dynamic communication topology," *Automatica*, vol. 80, pp. 261–271, 2017.

[13] P. Marti, M. Velasco, E. X. Martin, L. G. de Vicuna, J. Miret, and M. Castilla, "Performance evaluation of secondary control policies with respect to digital communications properties in inverter-based islanded microgrids," *IEEE Transaction on Smart Grids*, vol. 99, September 2016.

[14] J. Schiffer, C. A. Hans, T. Kral, J. Raisch, and R. Ortega, "Modelling, analysis and experimental validation of clock drift effects in low-inertia power systems," *IEEE Transactions on Industrial Electronics, Special Section on Power-Electronics-Enabled Autonomous Power Systems*, 2017.

[15] J. Schiffer, R. Ortega, C. A. Hans, and J. Raisch, "Droop-controlled inverter-based microgrids are robust to clock drifts," in *ACC*, June 2015, pp. 2341–2346.

[16] C. D. Godsil and G. F. Royle, *Algebraic Graph Theory*. Springer, 2001, vol. 207.

[17] M. Mesbahi and M. Egerstedt, *Graph Theoretic Methods in Multiagent Networks*. Princeton University Press, 2010.

[18] P. Kundur, *Power system stability and control*. McGraw-Hill, 1994.

[19] A. J. Wood, B. F. Wollenberg, and G. B. Sheblé, *Power generation, operation and control*. IEEE Wiley, 2014.

[20] C. A. Hans, P. Sopasakis, A. Bemporad, J. Raisch, and C. Reincke-Collon, "Scenario-based model predictive operation control of islanded microgrids," *54th IEEE Conference on Decision and Control (CDC)*, p. 32723277, 2015.

[21] J. Schiffer, R. Ortega, A. Astolfi, J. Raisch, and T. Sezi, "Conditions for stability of droop-controlled inverter-based microgrids," *Automatica*, vol. 50, no. 10, pp. 2457–2469, 2014.

[22] J. H. Alimeling and W. P. Hammer, "PLECS-piece-wise linear electrical circuit simulation for simulink," in *IEEE PEDS*, vol. 1, 1999, pp. 355–360 vol.1.

APPENDIX I
REMARK ON SECONDARY CONTROL LAW

In the following we illustrate how the secondary controller in [10] is related to (20). In [10], (47), droop control at node i is described as

$$\omega_i = \xi_i - k_i P_i, \tag{27}$$

which can be transformed into (5b) with ω^d and P^d set to zero and considering a model without clock drifts. The secondary frequency control law proposed in (52), (53) in [10] can be expressed in our notation as

$$\dot{\xi}_i = -m_i\big(\textstyle\sum_{j\in\mathcal{J}} a_{ij}(\omega_i-\omega_j)+ n_i(\omega_i-\omega^d)+\sum_{j\in\mathcal{J}} a_{ij}(k_iP_i-k_jP_j)\big).$$

Inserting (27) yields

$$\dot{\xi}_i = -m_i\big(\textstyle\sum_{j\in\mathcal{J}} a_{ij}(\omega_i-\omega_j)+n_i(\omega_i-\omega^d)+ \sum_{j\in\mathcal{J}} a_{ij}((\xi_i-\omega_i)-(\xi_j-\omega_j))\big),$$

which is equivalent to

$$\dot{\xi}_i = -\big(m_in_i(\omega_i-\omega^d)+m_i\textstyle\sum_{j\in\mathcal{J}} a_{ij}(\xi_i-\xi_j)\big).$$

For $m_in_i = b_i$ and $m_i = d_i$ this equals (20).